

ChemComm

Accepted Manuscript



This is an *Accepted Manuscript*, which has been through the Royal Society of Chemistry peer review process and has been accepted for publication.

Accepted Manuscripts are published online shortly after acceptance, before technical editing, formatting and proof reading. Using this free service, authors can make their results available to the community, in citable form, before we publish the edited article. We will replace this *Accepted Manuscript* with the edited and formatted *Advance Article* as soon as it is available.

You can find more information about *Accepted Manuscripts* in the [Information for Authors](#).

Please note that technical editing may introduce minor changes to the text and/or graphics, which may alter content. The journal's standard [Terms & Conditions](#) and the [Ethical guidelines](#) still apply. In no event shall the Royal Society of Chemistry be held responsible for any errors or omissions in this *Accepted Manuscript* or any consequences arising from the use of any information it contains.

Developments and sensing applications of fluorescent motifs within mitochondrial environment

Roopa, Naresh Kumar, Vandana Bhalla* and Manoj Kumar*

Received 00th January 20xx,
Accepted 00th January 20xx

DOI: 10.1039/x0xx00000x

www.rsc.org/

The potential use of fluorescent molecular probes to measure ions and biomolecules contributed incessantly to the understanding of chemical and biological systems. The approach has many advantages, such as high sensitivity, simplicity and non-destructive cellular imaging that offers visible information about the targeted species. In this article, our objective is to discuss fluorescent probes that have sensing applications within mitochondrial environment. Mitochondria are cellular organelles which are well known for their unique physiological functions and have been found to be associated with various diseases and disorders. It is therefore, important to develop new tools and tactics that can provide useful information concerning mitochondrial environment which in turn is essential to understand its biophysical functioning and related diseases.

1. Introduction

Mitochondria, because of their physiological functioning, are organelles of particular interest found in the cytoplasm of almost all eukaryotic cells.¹ Although, the number, size and morphology of mitochondria vary from organism to organism, their structural composition is usually same. Mitochondria play significant roles in a variety of biological processes. The principal function of mitochondria is the energy production in the form of adenosine triphosphate (ATP), and hence are known as cellular power plants.² In addition, they regulate the cytosolic calcium homeostasis, cellular redox state, initiation of apoptosis and generation of reactive oxygen species.^{3,4} Mitochondrial dysfunction affects the body homeostasis and causes neurodegenerative and neuromuscular disorders. For

instance, the production of ATP is associated with the generation of reactive oxygen species (ROS) as a side product. These ROS cause oxidative stress responsible for the origin of numerous diseases including cancer, diabetes, obesity, and ageing.^{5,6} Though, mitochondria perform important physiological functions, but they are also linked with diseases and disorders. Thus, it is crucial to have sufficient knowledge concerning the physiological functioning and related defects of mitochondria which can be associated to available tools and tactics that can target mitochondria in the cellular environment. More attention is, therefore given to the development of sensitive techniques/systems that can identify and monitor the functioning of mitochondria.

A number of biological techniques such as radioisotope labelling, positron emission tomography and magnetic resonance imaging are available for monitoring the behaviour of biomolecules.⁷ However, fluorescence microscopy takes the advantages for its high sensitivity and high spatial resolution over the other analytical methods.^{8,9} Moreover, fluorescence imaging is an ideal technique for examining intracellular

Department of Chemistry, UGC-Center for Advanced Studies-1, Guru Nanak Dev University, Amritsar-143005, Punjab, India.
Tel.: +91-(183)-2258802-9 Extn. 3205; fax: +91-(183)-2258820;
E-mail: vanmanan@yahoo.co.in; mksharma@yahoo.co.in



Roopa was born in India in 1984. She received her bachelor's and master's degree (Hons. School) from the Department of Chemistry at Guru Nanak Dev University, Amritsar, India in 2007. She joined the research group of Dr. Vandana Bhalla and completed her doctoral degree in 2012 from Guru Nanak Dev University, Amritsar, India. Her main research focus on the design, synthesis of fluorescent receptors for species of environmental and biological importance.

Naresh Kumar belongs to Shahtalai, a small town in Himachal Pradesh, India. He completed his BSc from H.P. University, Shimla, and moved to Guru Nanak Dev University, Amritsar, India for MSc-Chemistry in 2007. He joined the research group of Prof. Manoj Kumar in the same University, as a PhD fellow in 2010. Presently, he is working with Dr. Isabelle Leray as a postdoctoral fellow at PPSM, ENS-Cachan, France. His research includes the macrocyclic hosts systems, fluorescent energy transfer systems for ions/molecules and their applications to bio-imaging.



molecules while minimally perturbing the cells, tissues and organisms.¹⁰ Therefore, these days fluorescent technique pooled with fluorescent probes have been widely used for real time visualization of molecules, ions and biologically relevant species in the solution and intracellular systems.¹¹⁻¹³ Though, the method is highly efficient, the design of fluorescent probe remains the governing factor for the success of the monitoring event. Usually, active sites that are able to interact with target are integrated with signalling units *i.e.* fluorophores to develop fluorescent probes. Further, fluorescent probes provide easily measurable photophysical changes particularly change in emission intensity and emission shifts while interacting with the analytes. Such types of changes have been attributed to the working of various photophysical mechanisms such as photo-induced electron transfer (PET), fluorescence resonance energy transfer (FRET), intramolecular charge transfer (ICT) and excimer or exciplex formation.¹⁴⁻¹⁶ Aggregation properties¹⁷ as well as spirocyclization¹⁸ have also been used to develop fluorescent systems. In addition, photophysical change induced by chemical reaction between fluorescent probe and analyte is also a unique tactic for the detection process.¹⁹

In this feature article, we primarily discuss fluorescent molecules designed and applied to target mitochondria with their particular applications to detect various species. The fluorescent probes have been categorized according to their sensing characteristics into different sections dealing with reactive oxygen species (ROS), metal ions, neurotransmitters, thiols and some miscellaneous examples (two-photon, mitochondrial matrix viscosity, pH etc.). The foremost purpose of this article is to outline the design approach and advancement of fluorescent probes targeting mitochondria along with their applications.

2. Mitochondrial targeting probes: Designs and tactics

The cellular respiration process offers a strong negative membrane potential (-180 mV) in the form of a proton gradient across the inner membrane of mitochondria.²⁰ The negative membrane potential of cellular mitochondria facilitates the

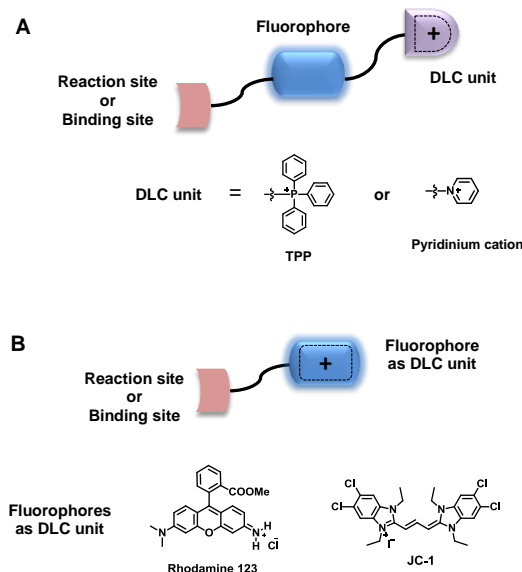


Fig. 1 Design of mitochondrial targeting fluorescent probes.

diffusion of cationic species towards the membrane over the anionic species. This feature of mitochondria distinguishes them from other organelles and provides opportunity to develop fluorescent probes that can selectively target the mitochondria. Among the various cations, especially, the lipophilic cations with delocalised positive charge (DLCs) effectively penetrate the hydrophobic barriers of phospholipid layer and mitochondrial matrix.²¹ The widely used fluorescent method involves the covalent linking of mitochondrial targeting group *i.e.* delocalized lipophilic cationic unit and binding site/reaction site to the fluorophore unit (Fig. 1A). The delocalized lipophilic cationic unit is connected to fluorophore unit *via* a flexible linker to separate it well from the fluorophore. Similarly, the binding/reaction site and lipophilic cation unit are separated as far apart to diminish interaction between them. The commonly used DLCs to target mitochondria are triphenylphosphonium (TPP) and pyridinium salts (Fig. 1A).²²⁻²⁴ These groups possess an overall positive charge which facilitates the permeation through plasma membrane into mitochondria of cell. Out of these lipophilic cations, TPP is explored widely as



Vandana Bhalla was born in Dhariwal (Gurdaspur), India in 1971. She received her Ph.D. from Department of Chemistry, Guru Nanak Dev University Amritsar and joined as a lecturer at B.B.K. D.A.V. College, Amritsar. She was JSPS fellow for two years at Tohoku University, Sendai, Japan and also worked in Aida Nanospace project as

JST researcher in Tokyo and then joined Department of Chemistry, Guru Nanak Dev University, Amritsar, India. She was a visiting scientist at University of Durham, UK in 2009 and 2013. Her area of research is functional materials. She has published around 135 research papers in international journals. She was conferred with Thomson Reuters Research Excellence India Citation awards in 2015.

2 | J. Name., 2012, 00, 1-3

Manoj Kumar studied chemistry at Guru Nanak Dev University, Amritsar, India and received his PhD in 1988. He has worked as a postdoc fellow at Instituto de Quimica Medica, Madrid, Spain. He was a visiting scientist at Johannes-Guttenberg University, Mainz, Germany and at Tohoku University, Japan. Currently, he is working as a professor at the Department of Chemistry, Guru Nanak Dev University, Amritsar. His research interest includes supramolecular host-guest chemistry of cyclic and acyclic receptors, fluorescent probes and liquid crystalline materials. He has published more than 140 research papers in international journals.



This journal is © The Royal Society of Chemistry 20xx

mitochondrial staining functional group due to its delocalized cationic π -system, geometry and rigidity.

Another method involves the use of fluorophore as DLC unit for mitochondrial localization which is covalently linked with the binding/reaction site (Fig. 1B). For instance, xanthenes (rhodamine 123) and cyanine based (JC-1) dyes as fluorescent lipophilic cations have been used for mitochondrial staining (Fig. 1B).²⁵ Therefore, these fluorescent protocols enable to monitor the changes which occur in the mitochondria due to alteration in the levels of reactive oxygen/nitrogen species, metal ions, thiols, pH, viscosity etc. by fluorescence imaging technique. In addition to these various other commercially available mitochondrial staining assays such as tetramethylrhodamine, MitoTracker®, MitoRed, MitoSOX™ etc. are also used to monitor mitochondrial structure, morphology and functioning.^{26,27} But, still there is need for the development of novel mitochondrial targeting fluorescent probes with improved properties such as large Stokes shifts, low cytotoxicity and excellent thermal, chemical and photostability. Moreover, designing probes that can exhibit bifunctional behaviour *i.e.* target mitochondria as well as able to provide information regarding their environment will be beneficial in all aspects.

3. Probes for mitochondrial reactive oxygen species

Reactive oxygen species (ROS) are short lived small molecules which execute varieties of physiological and pathological functions in living systems.^{28,29} These species are responsible for facilitating cell signalling and redox modification of various biomolecules. However, the increased level of ROS cause oxidative damage to biomolecules and hence is responsible for various diseases (Fig. 2). Mitochondria are the major source of cellular ROS that include hydrogen peroxide (H_2O_2), superoxide anion ($\text{O}_2^{\cdot-}$), hydroxyl radical ($\cdot\text{OH}$) and hypochlorite ion (ClO^-).^{30,31} Among all ROS, superoxide anion ($\text{O}_2^{\cdot-}$) is initially generated in the respiratory chain by the one electron reduction of O_2 following its fast reduction by superoxide dismutases (SODs) to H_2O_2 in the inter membrane space.³² H_2O_2 is a biologically prevalent ROS and serves crucial roles ranges from cell maintenance, survival, growth to

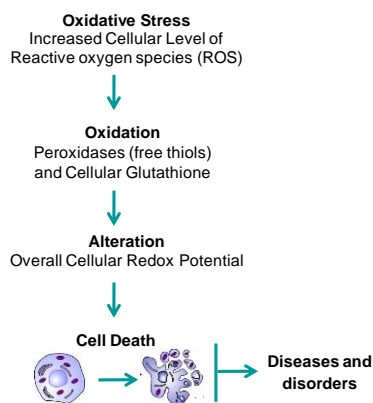


Fig. 2 Cell apoptosis induced by oxidative stress.

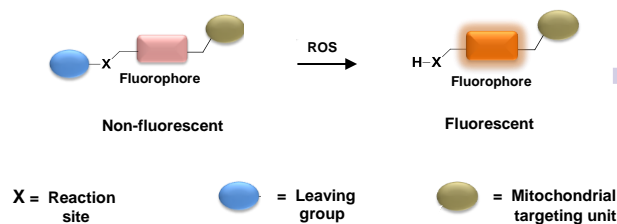


Fig. 3 ROS-induced fluorescence “Off-On” process.

serious physiological disorders.³³ The highly reactive ClO^- ion is associated with immune defence processes of cellular systems³⁴ but increased level is indicator of diseases, such as atherosclerosis, osteoarthritis and lung injury.^{35,36}

Therefore, development of fluorescent probes for dynamic and specific tracing of mitochondrial ROS has received extensive attention. The basic design of fluorescent probe for mitochondrial ROS is given in Fig. 3. Initially, the ROS sensitive probe is non-emissive in nature due to the photoinduced electron transfer (PET) or weak conjugation to the fluorogenic part in the excited state. However, after reaction with ROS, the cleavage of leaving group takes place which suppresses the PET effect or results in a highly conjugated system and the fluorescence of the probe is restored. For example, Nagano *et al.* reported mitochondrial targeting fluorescent probes **1a-b** for the detection of reactive oxygen species in living cells (Fig. 4).³⁷ The sensing systems comprised of rhodamine dye as a mitochondrial targeting unit appended with 4-amino or 4-hydroxyphenyl ether at the second position of phenyl moiety of rhodamine to facilitate the PET process. Probes **1a-b** undergo instantaneous fluorescent enhancement in an aqueous solution on reacting with highly ROS ($\cdot\text{OH}$, ONOO^- , OCl^-) due to the cleavage of ether moiety. HeLa cells imaging showed that probe **1a** is not sensitive to autoxidation and localizes selectively in mitochondria. Although, **1a** is able to monitor mitochondrial ROS in living cells, lack of selectivity for particular reactive oxygen species limits its practical application. In this context, Chang *et al.* reported a xanthenone based bifunctional probe **2** that combines boronate and triphenylphosphonium moieties as a H_2O_2 responsive and mitochondrial staining groups, respectively (Fig. 5).³⁸ In buffered solution of physiological pH, probe **2** exhibited a weak emission band at 540 nm ($\Phi = 0.019$) and undergoes fluorescence enhancement at ~ 528 nm ($\Phi = 0.405$) upon addition of H_2O_2 . This fluorescence enhancement was attributed to H_2O_2 -mediated boronate deprotection reaction which subsequently opens the lactone ring and forms a fully

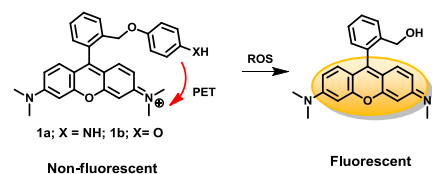


Fig. 4 PET based probes **1a-b** for mitochondrial ROS.

conjugated xanthenone dye. Colocalization experiments with MitoTracker showed that probe **2** stains mitochondria effectively and can detect the level of endogenous H_2O_2 in living cells with fluorescence turn-on response.

The one photon fluorescent probe limits the sensitive and selective imaging of mitochondrial reactive oxygen species in deep tissues due to background perturbation and shallow penetration depth. On the other hand, two-photon (TP) fluorescent probe provides advantages such as long-wavelength excitation, high resolution, less photo-damage and increased penetration depth.³⁹ Therefore, Kim *et al.* developed a TP fluorescent probe **3** for the ratiometric detection of H_2O_2 in solution as well as within mitochondrial environment (Fig. 5).⁴⁰ Upon excitation at 370 nm, free **3** displayed fluorescence maxima at 470 nm in buffer solution. The addition of H_2O_2 resulted in the increase of emission intensity at 545 nm with a simultaneous decrease of fluorescence intensity at 470 nm. This Stokes shift is ascribed to the greater stabilization of the charge transfer excited state due to H_2O_2 -induced boronate cleavage that liberates a stronger electron-donating group. Probe **3** works in a physiological pH range with a detection limit of 4.6 mM for H_2O_2 . Moreover, **3** showed the TP spectral changes in response to H_2O_2 which followed a pseudo 1st-order kinetics with $k_{\text{obs}} = 1.0 \times 10^{-3} \text{ s}^{-1}$ and resulted in a 40-folds enhancement in the $F_{530-600}/F_{400-470}$ ratio. Further, cellular studies inferred that probe **3** localizes in mitochondria and can ratiometrically monitor the changes of mitochondrial H_2O_2 in live cells as well as in living tissues at 100-180 μm depth. Tang *et al.* reported TP fluorescent probe **4** by utilizing benzothiazoline receptor and TPP salt for imaging superoxide ion ($\text{O}_2^{\cdot-}$) in mitochondria.⁴¹ On reacting with $\text{O}_2^{\cdot-}$ probe **4** undergoes remarkable fluorescence enhancement at 512 nm, ascribed to $\text{O}_2^{\cdot-}$ triggered benzothiazoline dehydrogenation which increases the conjugation of the system. The one photon spectra of **4** showed linear fluorescence enhancement through $\text{O}_2^{\cdot-}$ concentrations with the detection limit of 9.5 nM. Live cell imaging experiments of probe **4** showed low cytotoxicity, no photobleaching, preferential mitochondrial accumulation and can detect the rise of intracellular $\text{O}_2^{\cdot-}$ levels. Further, *in vivo* imaging validate the applicability of this probe for monitoring fluctuations in $\text{O}_2^{\cdot-}$ levels in living cells.

Li *et al.* reported fluorescent probes **5a-b** for detecting mitochondrial hypochlorite ions.⁴² In probes **5a-b** rhodamine moiety is linked with TPP and pyridinium units, respectively as

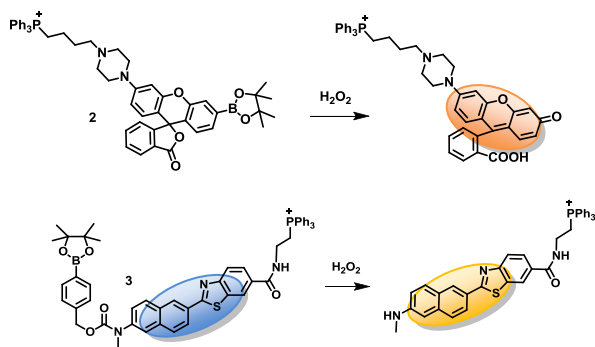


Fig. 5 H_2O_2 -mediated fluorescence changes in **2** and **3**.

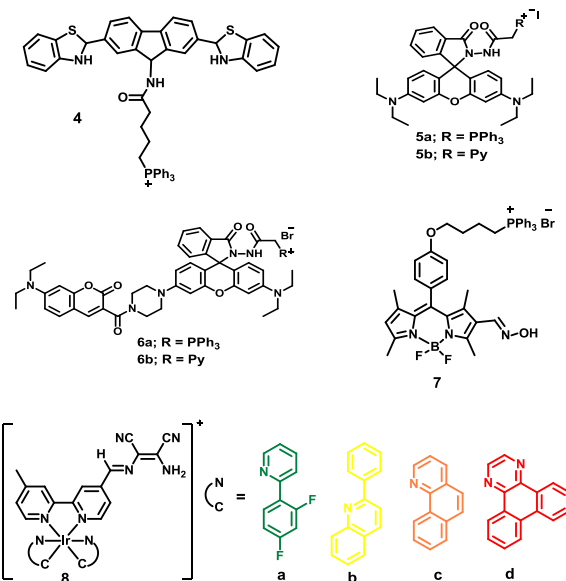


Fig. 6 Structures of compounds **4-7** and **8a-d**.

mitochondria-targeted functional groups. The addition of NaClO to the solution of **5a** and **5b** gave 200 and 380-folds fluorescence enhancement, respectively which is attributed to the ClO^- -induced oxidation-hydrolysis of benzoyl acetohydrazide moiety. Both probes showed selectivity toward ClO^- over other ROS as well as cations and the detection limits were found to be $1.1 \times 10^{-7} \text{ M}$ and $2.4 \times 10^{-8} \text{ M}$, respectively. Cellular imaging and *in vivo* experiments revealed that both probes are cell permeable, localize in mitochondria and can rapidly monitor the intracellular ClO^- . Moreover, it was found that the probe **5b** having pyridinium group caused less damage to HeLa cell. The same group further reported probes **6a-b** based on the combination of coumarin-rhodamine dyads appended with TPP and pyridinium units, respectively for the ratiometric and selective detection of ClO^- .⁴³ It has been observed that the probe **6a** is efficient to differentiate normal and cancer cell on the basis of mitochondrial ClO^- levels.

Fan *et al.* developed fluorescent probe **7** based on the $\text{C}=\text{N}$ isomerization mechanism for detecting ClO^- in the living cells.⁴⁴ In the probe design, oxime group was attached on the 2-position of BODIPY core and triphenylphosphonium group was introduced at the *meso*-position of the probe. Free **7** exhibited absorption maximum at 518 nm in mixture of PBS buffer and EtOH (1/9, v/v). The addition of NaClO to the solution of **7** shifted the absorption maxima to lower wavelength along with color change from pink to yellow, while the fluorescence spectrum showed 35-folds fluorescence enhancement at 520 nm. Further, the reported sensor works over a broad pH range (3-13) and exhibited no interference from other reactive species. *In vitro* experiments demonstrated that probe **7** selectively localized in mitochondria and rapidly reacts with ClO^- in living cells. Recently, Chao *et al.* utilized Ir(III) complexes **8a-d** for the selective detection of ClO^- ions in aqueous solution and for the imaging of mitochondrial ClO^- in cells.⁴⁵ Initially, complexes **8a-d** exhibited weak emission in

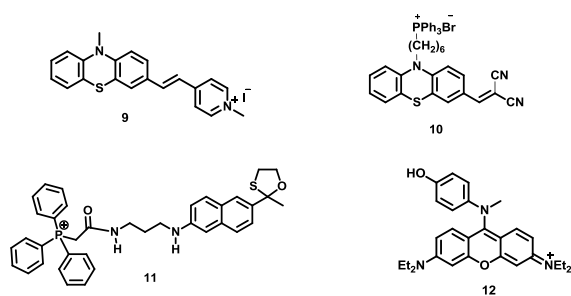


Fig. 7 Structures of compounds 9-12.

the range of 534-598 nm owing to the presence of C=N bond which enables non-radiative decays of excited state fluorophores. On reacting with ClO^- , these complexes undergo significant phosphorescent enhancement attributed to the inhibition of non-radiative decay process assisted by the conversion of diaminomaleonitrile moiety into carboxylate group. The cellular studies revealed that probes **8a-d** maintain low cytotoxicity, 70% localization in mitochondria and detect endogenous ClO^- generated *via* enzymatic reactions in the living cells.

Yin and coworkers reported fluorescent probes **9**⁴⁶ and **10**⁴⁷ for the detection of mitochondrial ClO^- where pyridinium and TPP units, respectively, were used to target mitochondria. In case of **9**, oxidation of divalent sulphur by NaClO has been employed to obtain fluorescence change. On the other hand, probe **10** exhibited ratiometric fluorescence change owing to the breaking of C=C bond promoted by oxidation of NaClO . Chang *et al.* developed two photon based probe **11** for the selective detection and imaging of mitochondrial HClO .⁴⁸ Imaging studies data showed that probe **11** favourably target the mitochondria of cell and able to detect HClO within nanomolar range. Recently, a highly responsive fluorescent probe **12** based on methyl(4-hydroxyphenyl)amino-substituted pyronin has been reported by Guo *et al.* for measuring the exogenous/endogenous level of ONOO^- ions in cellular mitochondria.⁴⁹ In solution, **12** did not exhibit any emission as PET process take place from the methyl-(4-hydroxyphenyl)amino group to the excited fluorophore. However, the addition of ONOO^- ions resulted in the formation of fluorescent aminopyronin. Likewise, imaging experiments confirmed the cell penetrating and mitochondrial ONOO^- staining ability of probe **12**. Similarly, Han *et al.* synthesized fluorescent probe **13** based on cyanine dye to monitor the level of ONOO^- in cellular systems and solution.⁵⁰ The weak fluorescence emission of probe **13** at 820 nm ($\Phi = 0.0032$) showed significant enhancement ($\Phi = 0.0431$) with the addition of ONOO^- ions. This is ascribed to the oxidation of probe **13** by

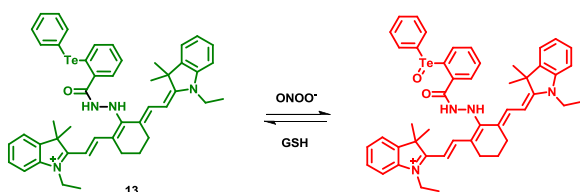


Fig. 8 Fluorescence changes in **13** with ONOO^- and GSH.

peroxynitrite (Fig. 8). The real time imaging studies proved the localization of probe within mitochondria. Further, the redox reversibility of **13** with ONOO^- and GSH has been also confirmed in the solution as well as in the mitochondrial environment. Apart from above reports, a nanoprobe based on micelle system having FRET donor-acceptor groups has been developed recently for the ratiometric detection of exogenous/endogenous mitochondrial H_2O_2 .⁵¹

From the above discussion, it is clear that the target specific fluorescent probe is an appropriate and simple approach to visualize the generation and accumulation of mitochondrial reactive oxygen species *in vivo* and *in vitro*. However, there are only a handful of fluorescent probes are available to monitor the mitochondrial ROS and some of them encounters poor water solubility as well as interference from other reactive oxygen species. Moreover, all fluorescent probes showed emissions in the range of 512-590 nm which constraints their imaging applications. Thus, there is a special requisite to develop novel fluorescent motifs which have emissions in the NIR region, good water solubility and selectivity towards particular mitochondrial ROS.

4. Probes for mitochondrial metal ions

Transition metal ions are important for a wide range of biological processes as they are present within organelles as cofactors of metalloenzymes and metalloproteins.^{52,53} Among various metal ions, iron is the most abundant transition metal ion in the human body. It is present in mitochondrial Fe-S centers and hemoproteins, performs various physiological functions such as oxidation-reduction reactions, oxygen metabolism and DNA synthesis.⁵⁴ However, imbalance of mitochondrial Fe-S clusters leads to the blood disorders and mitochondrial iron overloads which in turn generate ROS and ultimately results in the toxic effects.^{55,56} Thus, the development of selective fluorescent probe for quantification of iron in mitochondria is utmost important. In this context, Ning *et al.* reported a FRET based ratiometric fluorescent probe **14** for detection of mitochondrial Fe^{3+} ions. In the design, rhodamine moiety is conjugated to naphthalene and TPP as organelle targeting unit.⁵⁷ Probe **14** gave naphthyl emission at 431 nm, when irradiated at 371 nm. The addition of Fe^{3+} led to the decrease in emission intensity at 431 nm along with enhancement in emission at 594 nm. This process is attributed to energy transfer from the conjugated naphthalene donor to the ring-opened rhodamine acceptor. The reported probe is highly

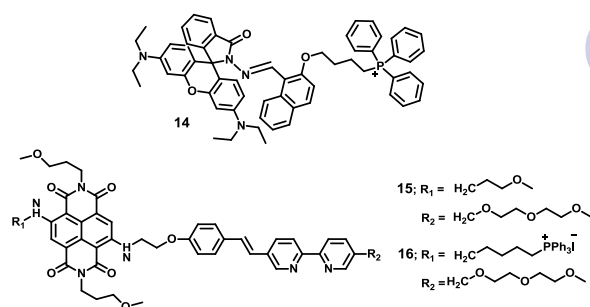


Fig. 9 Structures of compounds 14-16.

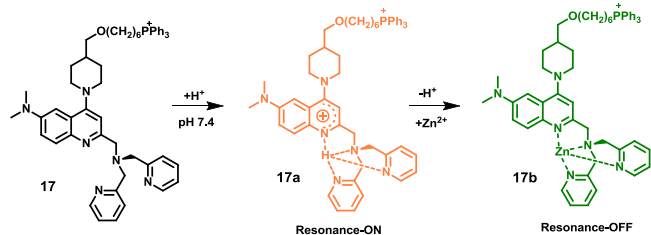


Fig. 10 Zn^{2+} -mediated ratiometric fluorescence changes in **17**.

selective for Fe^{3+} ions with a detection limit of 6.93×10^{-6} M. The method of continuous variations (Job's plot) indicated a 1:1 (host:guest) stoichiometry and the stability constant of the **14**- Fe^{3+} complex was found to be $(2.0 \pm 0.1) \times 10^4$ M^{-1} . Biological studies showed that **14** have ability to detect mitochondrial Fe^{3+} in cells by FRET mechanism.

Zinc is another abundant and vital trace element in human body required for intracellular signaling, protein synthesis and enzyme activity.⁵⁸ In mammalian cells, around 95% of intracellular zinc complexed to peptides and enzymes, while only small amount of zinc exists as in the free and exchangeable form.^{59,60} The secretory glands such as pancreas, prostate, and mammary glands regulate zinc secretion for critical biological processes within the body. However, alteration of zinc homeostasis causes health disorders.⁶¹ Moreover, increased concentration of intra mitochondrial zinc can promote mitochondrial dysfunction and generation of ROS.^{62,63} In order to understand Zn^{2+} biology, sincere efforts have been devoted to develop mitochondrial Zn^{2+} targeting fluorescent probes. Zhu *et al.* reported resonance energy transfer based probes **15** and **16** for the detection of Zn^{2+} ions in solution as well as in living cells.⁶⁴ Probe **15** consists of bipyridine and naphthalenediimide (NDI) derivatives as FRET donor-acceptor pair, whereas **16** also have a TPP moiety as a mitochondrial staining functional group. Probe **15** showed a weak fluorescence emission at 630 nm, when excited at 400 nm. Upon addition of Zn^{2+} ions the emission band undergoes 12-folds enhancement in CH_3CN . However, in a mixed organic solvent **15** showed only 3-folds fluorescence enhancement. These changes are ascribed to Zn^{2+} -coordinated energy transfer process from bipyridine donor derivative to NDI core. Further, colocalization experiments of these probes with commercially available MitoTracker fused with cyan fluorescent protein revealed that **16** stain mitochondria selectively due to the presence of TPP group. In addition, probe **16** exhibited little pH sensitivity within the physiological window and acts as a ratiometric sensor for mitochondrial zinc ions.

Jiang *et al.* developed quinolone based fluorescent sensor **17** for ratiometric detection of mitochondrial zinc ions (Fig. 10).⁶⁵ In probe **17**, quinolone moiety is linked with picolylamine and TPP salt for selective Zn^{2+} binding and effective mitochondrial staining. Free **17** showed fluorescence emission at 550 nm ($\Phi = 0.11$) in HEPES buffer at pH 7.4. The addition of Zn^{2+} ions leads to fluorescent enhancement at around 450-560 nm with simultaneous decrease of fluorescence emission at

around 570-670 nm along with a significant hypsochromic shift of 46 nm. The fluorescence enhancement and emission shift arises due to the deprotection of quinolinic site on Zn^{2+} coordination which subsequently inhibits resonance process occurring in the molecule (Fig. 10). Further, imaging experiments showed that probe **17** have low cytotoxicity, pH insensitivity, and colocalization coefficient of 0.86 with MitoTracker and can selectively monitor the changes of intracellular Zn^{2+} concentration *via* ratiometric approach.

Kim *et al.* reported a two photon probe **18** for the detection of Zn^{2+} ions having 6-(benzo[d]thiazol-2'-yl)-2-(*N,N*-dimethylamino)naphthalene as a reporter, *N,N*-di-(2-picolyl)-ethylenediamine as the Zn^{2+} binding site and TPP as the mitochondrial-targeting unit.⁶⁶ Probe **18** exhibited fluorescence emission band at ~ 500 nm ($\Phi = 0.15$) and undergoes gradual red shifts (45 nm) with increasing the polarity of solvent. The addition of Zn^{2+} ions resulted in fluorescence enhancement at ~ 490 nm ($\Phi = 0.92$). This change is attributed to inhibition of the PET process as well as to the decreasing electron donating ability of the amino group owing to **18**- Zn^{2+} complex formation. Further, Job's plot indicated a 1:1 (host:guest) stoichiometry and detection limit of 3.1 nM for Zn^{2+} ions. The reported probe showed TP action cross section of 75 GM at 750 nm in the presence of excess Zn^{2+} , low cytotoxicity and effective mitochondrial localization in living cells. Apart from this, rat hippocampal tissue imaging revealed that the probe can selectively monitor intra-mitochondrial Zn^{2+} at a depth of 100-200 μm . However, probe **18** undergoes only 7-fold fluorescence enhancement in the presence of excess Zn^{2+} ions. Thus, for more sensitive detection of mitochondrial Zn^{2+} , the same group further developed a sensitive two-photon fluorescent probe **19** which exhibited a 70-folds fluorescence enhancement in the presence of Zn^{2+} ions and 80 nm of emission shift with increasing solvent polarity.⁶⁷ Probe **19** showed TP action cross section of 155 GM in the presence of excess of Zn^{2+} ions and detect mitochondrial Zn^{2+} in live cells and tissues with a brighter and clearer TPM image without interference from other metal ions. Recently, another two photon chemosensor **20** was developed by Cho *et al.* for the detection of mitochondrial zinc ions in live cells and tissues.⁶⁸ Only the addition of Zn^{2+} ions to the buffer solution of **20** gave

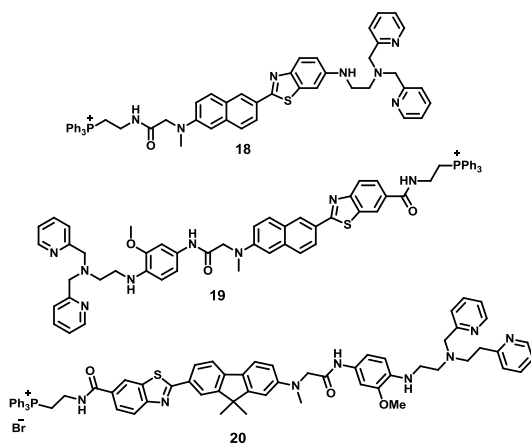


Fig. 11 Structures of compounds **18-20**.

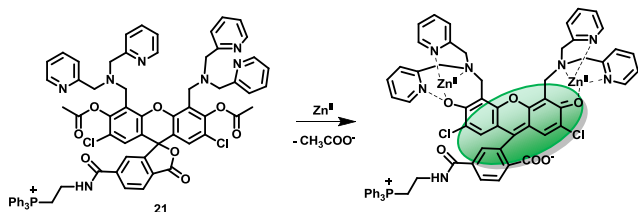


Fig. 12 Zn^{2+} -mediated hydrolysis of **21**.

dramatic TP excited fluorescence enhancement at 559 nm due to inhibition of PET process. Job's plot confirms the 1:1 (host:guest) stoichiometry and the dissociation constant of the **20**- Zn^{2+} complex in a TP mode was found to be 17 ± 2 nM. The TPM and colocalized images of the HeLa cells showed that probe preferably target mitochondria.

Lippard *et al.* developed a reaction based fluorescent probe **21** for monitoring mitochondrial mobile Zn^{2+} ions within the cells (Fig. 12).⁶⁹ Initially, probe **21** did not exhibit any fluorescence emission due to the presence of acetyl group on phenolic oxygen atoms of xanthene ring which results in formation of lactone ring. The addition of Zn^{2+} ions caused hydrolysis of the ester groups which ultimately opens the lactam ring of xanthene moiety and gave 140-folds fluorescence enhancement at 529 nm. In addition, probe **21** showed partial reversibility with EDTA due to PET from the dipicolylamine to xanthene moiety. Probe **21** was found to be localizing in the mitochondria of living cells and monitor mobile intracellular zinc ions. The same group also reported resorufin based probes **22** and **23** for detecting mobile zinc ions in solution as well as in living cells.⁷⁰ Compounds **22** and **23** exhibited weak fluorescence emission at 630 nm and 611 nm, respectively in aqueous buffer solution. The addition of excess of Zn^{2+} gave 14 and 41-folds fluorescence enhancements, respectively. Probe **23** showed binding affinity of nanomolar range for zinc ions and non-linear plot demonstrated dissociation constant of 3.25 ± 0.12 nM. Biological studies revealed that **22** and **23** are cell permeable and can be used for intracellular zinc imaging.

Copper is another essential metal ion present within mitochondria matrix and inner-membrane space as a cofactor of cytochrome c oxidase (CcO) and superoxide dismutase (SOD1)

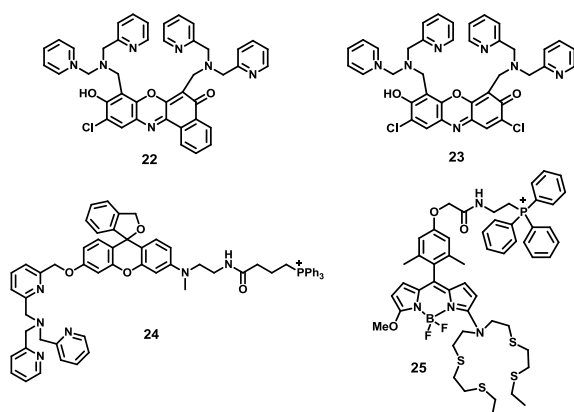


Fig. 13 Structures of compounds **22**-**25**.

enzymes. The copper containing CcO enzyme plays an important role in the generation of ATP as it acts as electron acceptor in the mitochondrial electron chain, whereas, SOD1 enzyme is involved in the free radical detoxification process.⁷¹ However, the high redox reactivity of copper can cause toxicity to the cell due to the generation of ROS as well as displacing other metal cofactors from their natural ligands. This arouses the interest for the monitoring of copper ions in the intracellular environment. Taki *et al.* developed a rhodol-based fluorescent probe **24** for the detection of mitochondrial copper ions.⁷² Free **24** showed weak fluorescence emission at 542 nm due to the cyclization of hydroxymethyl group. The addition of Cu^+ leads to 100-folds fluorescence enhancement owing to the Cu^+ -mediated cleavage of C-O bond of benzyl ether, resulting in the formation of fluorescent ring-opened species. Further, the stained subcellular localization and imaging experiments elucidated that **24** is certainly localized to mitochondria and suitable to monitor mitochondrial Cu^+ in copper supplemented cells. Chang *et al.* reported a bifunctional reporter **25** which combines a Cu^+ sensitive fluorescent platform with a mitochondrial-targeting TPP moiety for imaging exchangeable mitochondrial copper pools in living cells.⁷³ Probe **25** exhibited a poor fluorescence emission at 569 nm ($\Phi = 0.009$) in aqueous media buffered to physiological pH. The addition of Cu^+ ions to the solution of probe gave 10-folds ($\Phi = 0.05$) fluorescent enhancement along with 11 nm blue shift. The binding analysis using the method of continuous variations (Job's plot) indicated 1:1 stoichiometry with stability constant of 7.2×10^{12} M⁻¹. Confocal microscopy experiments showed that **25** can detect changes in labile mitochondrial Cu^+ concentration. Likewise, **25** in conjunction with biochemical and ICP metal analysis revealed that the alterations in mitochondrial metallochaperone did not change exchangeable mitochondrial Cu^+ or total mitochondrial Cu pools relative to control cells.

The examples discussed above evidently specify that the mitochondrial targeting fluorescent probe is a powerful tool for real time visualization of metal homeostasis at the cellular level. Although a good number of fluorescent probes have been developed for *in vivo* imaging but there is still lacking of certain factors such as long wavelength emission, brightness, fluorophore stability and probe pharmacokinetics.

5. Probes for mitochondrial gasotransmitters

Gasotransmitters, as the name indicates are small gaseous molecules that execute distinctive signal functioning in the cellular system. For example, nitric oxide (NO), the active member of reactive nitrogen species is generated endogenously in cells during the conversion of L-arginine to L-citrulline by nitric oxide synthases (NOS).^{74,75} NO acts as an intra- and extracellular messenger, involved in a wide range of biological processes such as cardiovascular, immune, and the central and peripheral nervous systems.^{76,77} The lower level of NO encourages protective effect on cells, while its higher level promotes the production of other reactive species such as $ONOO^-$, N_2O_3 , NO_2^- , and NO_3^- responsible for various pathophysiological diseases.^{78,79}

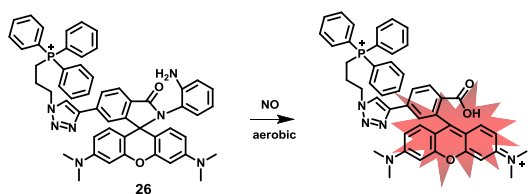


Fig. 14 NO-induced spirolactam ring-opening process in 26.

The endothelial NOS is a unique isoform of NOS which is involved in the production of NO within the mitochondria of endothelial and neuron cells.⁸⁰ Nitric oxide controls the various functions of the mitochondria such as oxygen supply to the mitochondria by regulating the oxygen binding or release from haemoglobin and inhibiting the enzyme actions to control the functions of the mitochondria.⁸⁰ The utilization of fluorescent probes for visualizing NO activity and signalling mechanisms in the mitochondria of living cells showed its importance in the biological systems. Xiao *et al.* reported a fluorescent probe **26** for the detection of NO in solution and in the mitochondria of living cells (Fig. 14).⁸¹ The authors utilized rhodamine spirolactam as a NO signaling moiety and TPP as mitochondrial directing unit. Probe **26** upon reaction with NO exhibited 60-folds fluorescence enhancement at 585 nm, attributed to NO-induced spirolactam ring-opening reaction of rhodamine moiety. Probe **26** showed selectivity towards NO over other reactive oxygen/nitrogen species and the detection limit was found to be 4.0 nM. Intracellular studies showed that **26** possesses less toxicity at low concentration, pH insensitivity and high colocalization coefficient with commercially available MitoTracker indicating that this probe localized specifically in mitochondria. Further real time imaging experiments indicated that **26** can effectively detect endogenous and exogenous NO in mitochondria of living cells.

Nitric oxide mediated cyclization of *o*-phenylenediamino moiety to form fluorescent benzotriazole derivative *via* blocking of photo-induced electron transfer process has been an appropriate approach for imaging of NO in living cell (Fig. 15a).⁸²⁻⁸⁴ However, the proton present on benzotriazole moiety may interfere with the NO detection sensitivity at physiological pH as its deprotonation can cause the fluorescence quenching *via* PET process. Keeping this in mind, Guo *et al.* developed mitochondria targetable fluorescent probe **27** in which pyronin dye is directly linked with one of the amino groups of *o*-phenylenediamino moiety for selective and sensitive detection

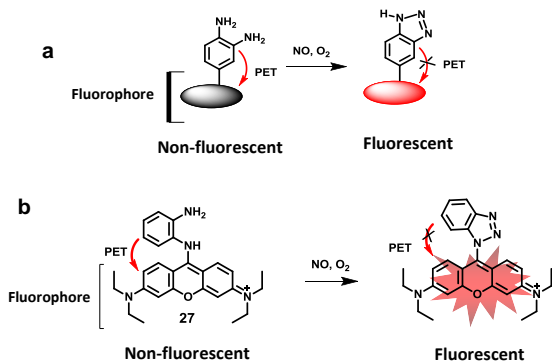


Fig. 15 NO-mediated diamine cyclization (a) general strategy (b) in 27.

of NO (Fig. 15b).⁸⁵ Free **27** exhibited negligible fluorescence emission at 616 nm owing to PET from *o*-phenylenediamine moiety to the excited pyronin moiety. The reaction of NO with **27** turns strong fluorescence enhancement ascribed to inhibition of PET process by triazole-ring formation. Probe **27** showed excellent selectivity for NO over other reactive oxygen/nitrogen species, dehydroascorbic acid and ascorbic acid as well as in the presence of biothiols, however, the addition of Cys/GSH to the solution of **27**-NO results in the formation of green-emission aminopyronin/red-emission thiopyronin. The biological studies revealed that probe **27** can monitor both exogenous and endogenous NO in dual-channel mode assisted by intracellular GSH and Cys. The similar strategy has been recently employed by Chao *et al.* to develop a two photon Ir(III) phosphorescence probe for the selective monitoring of mitochondrial NO.⁸⁶

The endogenously produced hydrogen sulfide (H_2S) is another important gaseous signaling molecule in cell system, generated from cysteine and its derivatives.⁸⁷ H_2S regulates a variety of physiological processes such as cell growth, vasodilation, antioxidation and anti-apoptosis effects.⁸⁸ However, variation in level of H_2S is the origin of various diseases like Alzheimer's disease, Down's syndrome and liver cirrhosis.⁸⁹ H_2S is usually produced in the cytosol by the action of cystathionine γ -lyase (CSE).⁹⁰ However, the stress conditions facilitate the translocation of cytosol CSE to the mitochondria for the production of H_2S . This H_2S production regulates the mitochondrial energy metabolism i.e. the synthesis of ATP by monitoring the level of oxygen.⁹⁰ Indeed, H_2S performs essential functions, and its high concentration inhibits the activity of the cytochrome c oxidase in mitochondria and is thus accountable for the decreased ATP synthesis. Therefore, to understand the distribution and activity of H_2S in biological systems, the development of technique to measure H_2S is essential. In this context, He *et al.* reported mitochondria targeting ratiometric fluorescent probe **28** based on coumarin-merocyanine scaffolds for cellular H_2S (Fig. 16).⁹¹ Probe **28** in PBS buffer is characterized by the two emission bands at 510 and 652 nm due to coumarin and merocyanine

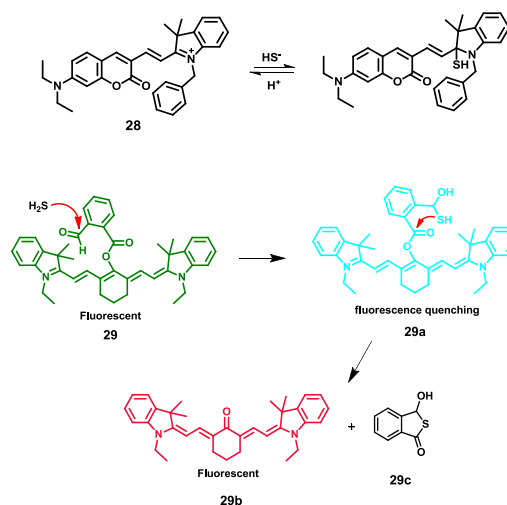


Fig. 16 Nucleophilic addition reaction of H_2S in **28** and **29** to induce fluorescence changes.

moieties, respectively. The addition of NaHS among the various anions, inorganic reactive sulfur species, biological thiols and reactive oxygen/nitrogen species resulted in the quenching of merocyanine emission at 652 nm with simultaneous enhancement of coumarin emission at 510 nm. The nucleophilic addition reaction of HS⁻ to the indolenium atom of probe **28** is responsible for this ratiometric change. Further, the real time imaging showed that probe preferentially localizes in mitochondria and can rapidly monitor the level of intracellular H₂S concentration.

Tang *et al.* reported a cyanine based fluorescent probe **29** for ratiometric detection of H₂S by using tandem nucleophilic addition-cyclization strategy (Fig. 16).⁹² The reaction of H₂S with **29** first results in fluorescence quenching at 780 nm which is ascribed to the nucleophilic addition reaction on the aldehyde group of **29** which enables PET process from the hydroxyl and sulfhydryl appended benzene ring to cyanine moiety. Further, the second nucleophilic addition on the ester moiety results in release of cyanine fluorophore. This fluorophore then undergoes tautomerism from enol to ketone form to emit at 625 nm. MTT and cell imaging experiments demonstrated that probe is of low toxicity, biocompatible, selectively localized into mitochondria of cell and can image the endogenously generated H₂S ratiometrically.

An azo-BODIPY based near IR probe **30** has been developed by Chen *et al.* for the detection of mitochondrial hydrogen polysulfides.⁹³ Free **30** did not exhibit any fluorescence emission as the d-PET process is operational from nitro-activated fluorobenzoate to the excited fluorophore. However, the addition of Na₂S₂ brought a 24-folds fluorescent enhancement at 730 nm owing to the cleavage of ester group which inhibits the d-PET process. Real time imaging studies revealed that probe **30** detects both exogenous and endogenous H₂S_n and can stain the mitochondria of cell as inferred from the colocalization experiments with rhodamine 123. Song *et al.* reported two photon fluorescent probe **31** derived from 1,8-naphthalimide as the fluorophore and 4-azidobenzyl carbamate as the H₂S reaction site for the ratiometric detection of mitochondrial H₂S.⁹⁴ The H₂S mediates the cleavage of carbamate which caused the reduction of azide to amine that switches a system for the ratiometric detection of H₂S. Probe displayed detection limit in nanomolar range of and exhibited good selectivity for H₂S over ROS and bithiols. The two-photon absorption cross section of the resulting species was found to be 218 GM which is greater than the probe **31**. Further, the probe showed lower toxicity, preferentially stain the mitochondria and can monitor the H₂S in cells by both one photon and two photon microscopy.

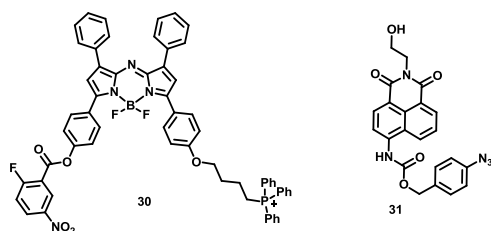


Fig. 17 Structures of compounds **30** and **31**.

6. Probes for mitochondrial thiols

Biothiols, namely cysteine (Cys), homocysteine (Hcy), glutathione (GSH) and thioredoxin (Trx) play vital roles in maintaining cellular redox homeostasis and protein functioning.⁹⁵ For example, GSH and Trx are primarily involved in maintaining mitochondria function by scavenging ROS.⁹⁶ The irregularities in the levels of thiols are associated with health problems.⁹⁷⁻⁹⁹ However, only few mitochondrial-targeted fluorescent probes capable of monitoring thiols inside living cells are known. Cho *et al.* reported naphthalene based probe **32** for ratiometric detection of mitochondrial thiols by using two-photon spectroscopy.¹⁰⁰ In the design, thiol reaction site *i.e.* disulfide bond and TPP salt as mitochondrial targeting unit are appended with naphthalene unit. The reaction of GSH with **32** in MOPS buffer gave new emission band at 545 nm with simultaneous decrease of fluorescence intensity at 462 nm. This is due to GSH-induced cleavage of C-N bond which in turn form more stabilised charge transfer excited state. Further, the probe works well in the wide pH range. The lower cytotoxic nature and a significant two-photon cross section of probe **32** favoured the mitochondrial localization as well as the capture of RSH levels in live cells. However, **32** also showed fluorescence response toward others thiols such as cysteine, dithiothreitol, 2-mercaptoethanol and 2-aminoethanethiol. Thus, for the selective detection of mitochondrial GSH, Kim *et al.* developed a NIR fluorescent probe **33** by using nitroazo unit as GSH-reaction site as well as the fluorescence quencher and delocalised heptamethine cation as the mitochondrial responsive unit.¹⁰¹ Initially, **33** exhibited small fluorescence emission at 764 nm ($\Phi = 0.001$), ascribed to the presence of nitroazo group which causes quenching *via* PET from cyanine to the nitroazo group. On reacting with GSH, the 1,6-conjugate addition of an alkyl thiol group on cationic receptor takes place along with cleavage of nitroazo group which resulted in drastic fluorescent enhancement at 810 nm ($\Phi = 0.187$) with a red shift from 764 nm to 810 nm. **33** was found to be selective with limit of detection of 26 nM for GSH. The confocal fluorescence images of living cells suggested that **33** can efficiently monitor the mitochondrial GSH level.

Kang *et al.* developed a fluorescent probe **34** for detecting mitochondrial Trx by introduction of both mitochondrial biomarker and Trx reaction site to the backbone of 1,8-naphthalimide moiety.¹⁰² The addition of Trx to the solution of

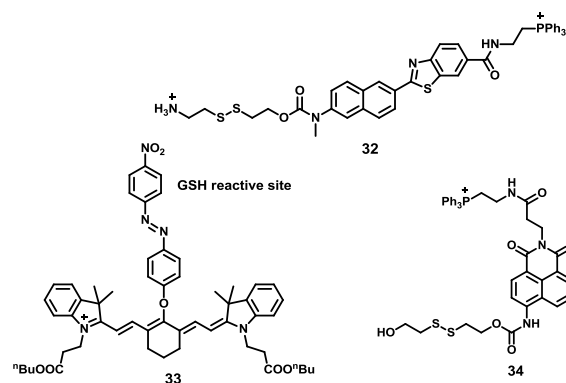


Fig. 18 Structures of compounds **32-34**.

34 under physiological conditions results in the appearance of green emission band at 540 nm with concurrent decrease of emission intensity at 472 nm, ascribed to the formation of more fluorescent species *via* Trx-mediated cleavage of disulfide bond of probe **34**. This process followed second-order kinetics with $k_2 = (4.04 \pm 0.26) \times 10^3 \text{ (M s)}^{-1}$ and the bond cleavage was 5000 times faster than that for GSH. Further, application to cellular imaging indicated that the probe was highly responsive to mitochondrial Trx compared with other biological thiols.

7. Probes for mitochondrial pH and viscosity

The ubiquitous pH values within the cellular organelles maintain and regulate the various biological processes such as apoptosis and ions transport.¹⁰³⁻¹⁰⁶ For example, within mitochondria the matrix sustains an alkaline pH under physiological conditions and generates proton-motive potential across the inner membrane.¹⁰⁷ This proton gradient is responsible for production of ATP as well as uptake of ion and metabolite into the matrix. At lower pH, mitochondrial depolarisation takes place which results in the alteration of calcium ion homeostasis.¹⁰⁸ In the past, various cytosolic pH sensors^{109,110} and genetically encoded pH sensors¹¹¹⁻¹¹³ such as green fluorescent protein, red fluorescent protein variants have been developed to monitor mitochondrial pH changes. However, they possess poor mitochondrial staining and their utilization in native cells is also limited. Recently, for imaging mitochondrial pH changes and pH-related physiological effects in live cells fluorescent probe **35** was developed by Sessler and coworkers.¹¹⁴ The fluorescent probe **35** comprises piperazine linked naphthalimide unit as fluorophore which is further associated with TPP and benzyl chloride as mitochondrial staining and fixation units, respectively. The authors exploited control compound **35a** to evaluate the pH effect which gave dramatic fluorescence enhancement at 525 nm by decreasing the pH from 11 to 2.0. The fluorescence enhancement occurs due to the presence of piperazine unit which gets protonated in acidic medium and inhibits photo-induced electron transfer (PET) process. Further, HeLa cell studies revealed that probe **35** possess low cytotoxicity, good mitochondrial staining and can be used to monitor pH changes within mitochondria related

with various pathogenic events. Moreover, **35** immobilized within the cells due to the nucleophilic substitution reaction of the benzyl chloride with endogenous thiols.

Tang *et al.* developed NIR fluorescent probe **36** based on π -conjugated system linked to the pH sensitive dimethylamino group for monitoring mitochondrial pH changes.¹¹⁵ At lower pH (2-4) in universal buffer solution, probe **36** showed minimum emission intensity as well as blue shift which is ascribed to the blockage of conjugation of system as the lone pair of nitrogen atom get protonated in acidic medium. On the other hand, at pH 8.0, probe **36** exhibited strong fluorescence emission at 680 nm. Further, imaging experiments proved that **36** effectively localize in mitochondria, possesses low cytotoxicity, good photostability and can visualize pH change in mitochondrial environment.

Intracellular viscosity plays key role in biological processes. For instance, diffusion of proteins and other bio-molecules within the cell membrane.¹¹⁶ The variation in cellular viscosity affects the functioning of lipid bilayer as well as rotation of biomolecules.¹¹⁷⁻¹¹⁹ Moreover, mitochondrial matrix viscosity is associated with the respiratory state of the mitochondria and thus viscosity measurement of mitochondrial environment is essential to understand the biophysical processes.¹²⁰ The rotor probes made significant contribution to investigate the intracellular viscosity. For example, Kang *et al.* developed a mitochondrial targeting viscosity probe **37** based on coumarin-BODIPY scaffold linked with a rigid phenyl spacer.¹²¹ Probe **37** exhibited very weak emission bands at 427 nm and 516 nm due to coumarin and BODIPY moieties, respectively in low viscosity medium. The weak emission arises due to free rotation around C-C bond of phenyl spacer and BODIPY moiety, which facilitate the non-radiative decay of excited state. With increasing solvent viscosity, BODIPY emission band at 516 nm undergoes more fluorescence enhancement as compared to the coumarin emission band at 427 nm. Further confocal laser fluorescence and fluorescence lifetime imaging experiments proved that **37** preferentially localize in the mitochondria and monitors the changes in mitochondrial viscosity which arises due to the presence of monensin or nystatin ionophore.

Peng *et al.* reported a carbazole modified cyanine base probe **38** for the fluorescence ratiometric measurement of mitochondrial viscosity *via* two-photon approach.¹²² Probe **38** has been found to be low emissive ($\Phi = 0.01-0.04$) at 580 nm in non-viscous solvents. However, it exhibits enhanced emission ($\Phi = 0.28$) at 580 nm upon increasing glycerol concentration. The cellular imaging studies confirmed the loading of **38** within the mitochondria. The probe is further employed for the viscosity measurement within the intracellular system and in tissues at depths of 60-130 μm using TPM. Similarly, Fan *et al.* developed two-photon fluorescent probe **39** for monitoring mitochondrial viscosity by using CHO group as molecular rotor.¹²³ Probe **39** showed 62.6 and 3.8-folds fluorescence enhancement at 658 nm and 467 nm, respectively by increasing the glycerol percentage in solvent mixture. This is owing to the viscosity-induced inhibition of CHO group rotation which disables non-radiative decay process from the excited state.

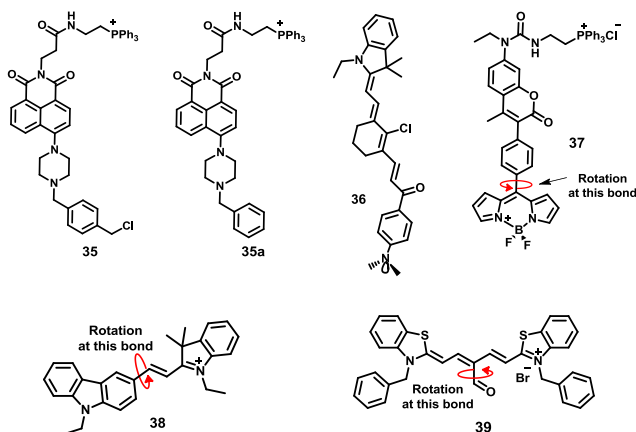


Fig. 19 Structures of compounds 35-39.

Moreover, by increasing solvent viscosity total fluorescence lifetime of probe at 658 nm also increased from 202.0 to 2374.3 ps conferred from fluorescence lifetime imaging. In addition, fluorescence imaging studies proved that **39** is bio-compatible and can monitor the viscosity changes within cellular mitochondria.

8. Miscellaneous probes

The increased level of superoxide ions in mitochondrion causes lipid peroxidation of its inner membrane which in turn damages proteins and mitochondrial DNA *via* disrupting oxidative phosphorylation process.¹²⁴ The elevated lipid peroxidation within the inner membrane is indicator of several pathologies. Thus, to monitor the level of lipid peroxidation in cellular mitochondria a peroxidation sensitive probe **40** was developed by Murphy and co-workers.¹²⁵ In the design, the backbone of BODIPY fluorophore is linked to both, a peroxidation sensitive group *i.e.* diene linker and TPP as mitochondrial targeting unit. In aqueous medium, **40** displayed emission bands at 515 nm and 545 nm and in ethanol one addition band appeared at 590 nm. On adding cumene hydroperoxide/CuSO₄, probe **40** undergoes oxidation and gave dramatic fluorescence enhancement at 520 nm with simultaneous decrease of fluorescence emission at 590 nm. The real time imaging studies showed that the probe is cell permeable, efficiently accumulate and ratiometrically analyse changes in mitochondria.

The excess of fluoride ions affects the energy generating efficiency and antioxidation activity of mitochondria by disturbing the glycolytic and citric acid cycle enzymes.¹²⁶ To monitor the level of fluoride ions, Peng *et al.* reported a mitochondrial targeting fluorescent sensor **41**.¹²⁷ The addition of F⁻ ions causes the cleavage of Si-O bond followed by intramolecular cyclization which gave fluorescent enhancement at 485 nm. The reported probe possesses low cytotoxicity, good mitochondrial staining and can easily visualize the level of fluoride ions with a strong green emission within cellular mitochondria.

Yu *et al.* reported carbazole-indolium based fluorescent sensor **42** for the ratiometric detection of SO₂ derivatives in solution and in cellular systems.¹²⁸ In solution, compound **42** exhibited emission band at 590 nm and the subsequent addition

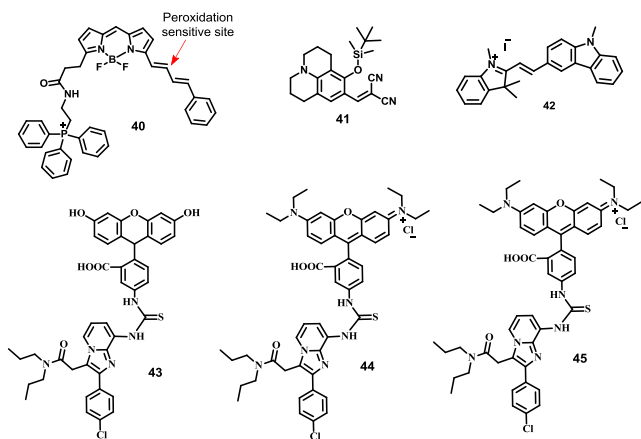


Fig. 20 Structures of compounds **40-45**.

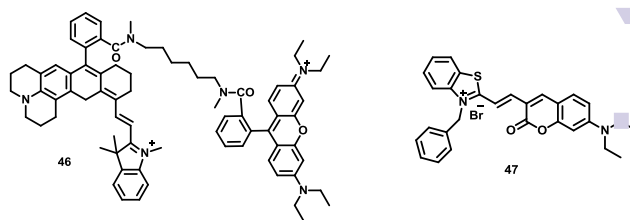


Fig. 21 Structures of compounds **46-47**.

of HSO₃⁻ resulted in the quenching of emission at 590 nm with the appearance of a new blue shifted emission band at 490 nm. Cellular imaging revealed that **42** offers lower cytotoxicity to cell and preferentially target the mitochondria attributed to the cationic indolium group. Denora *et al.* developed mitochondrial protein targeting fluorescent probes **43-45** for detecting activated microglia in living cells.¹²⁹

Takeoka *et al.* developed a ratiometric probe **46** which worked as a molecular thermometer both in solution and mitochondria of living cells.¹³⁰ The probe was found to show temperature dependent fluorescence change in mitochondria of cells, generated by exogenous heating. Fan *et al.* reported coumarin-hemicyanine based fluorescent probe **47** for the ratiometric monitoring of mitochondrial polarity.¹³¹ In MeOH, probe **47** showed two emission bands at 467 and 642 nm and exhibited ratiometric behavior on changing the polarity of solvent. The change in fluorescence intensity depends on the amount of energy released by excited state to become a more stable state. Wong *et al.* reported two-photon fluorescence probes **48a-b** based on carbazole-cyanine scaffold for imaging of mitochondria.¹³² The one and two-photon excited fluorescence images of living cell demonstrated that these probes localized selectively to the mitochondria of cells. Similarly, the other two-photon fluorescence probe **49** was developed by Kim *et al.* for real time imaging of mitochondrial trafficking by utilizing electron donor-acceptor architecture.¹³³ Recently, Yu *et al.* reported pyridine cation based probes **50-52** as mitochondrial staining compounds that possess larger TPA

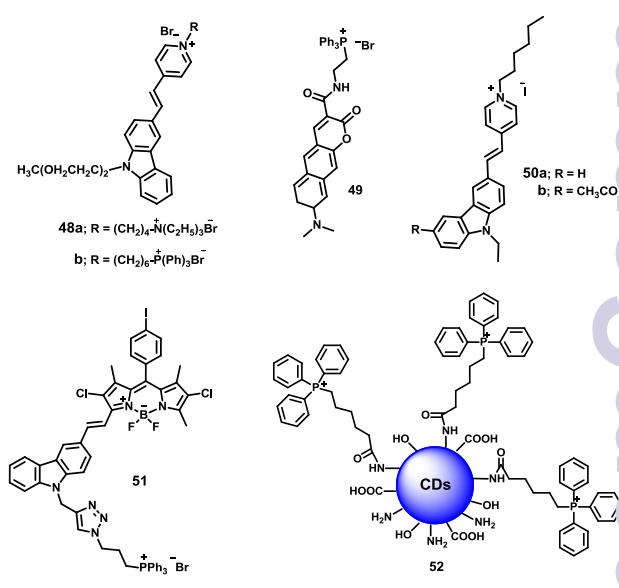


Fig. 22 Structures of compounds **48-52**.

cross section and stroke shifts than commercially available MitoTrackers.¹³⁴ The combination of BODIPY core and carbazole unit has also been used to develop NIR fluorescent probe **51** for mitochondrial imaging.¹³⁵ Ma *et al.* reported a bifunctional probe **52** containing both nitrogen-doped carbon dots as two photon fluorophore and TPP as a mitochondrial directing unit for selective imaging of mitochondria.¹³⁶

The high concentration of fluorescent probes such as rhodamines, BODIPY cyanines, naphthalimides restrict their application in mitochondria as they undergo self-quenching effect and also cause toxicity. Keeping this in mind, Tang *et al.* developed aggregation-induced emission (AIE) based probe **53** by utilizing tetraphenylethene scaffold for imaging mitochondria of cells.¹³⁷ Similar strategy was used by Liu *et al.* to develop a fluorescent probe **54** based on AIE phenomenon for mitochondrial staining.¹³⁸ Probe **54** did not exhibit any fluorescence emission in DMSO solution, but gave strong emission band at 532 nm in solid state with a 176 nm of Stokes shift. This emission enhancement is attributed to the restriction of intramolecular rotation around the N-N bond in the aggregated state and excited-state intramolecular proton transfer process. The real-time imaging studies demonstrated that **54** can monitor the mitochondria morphology and differentiation process of living brown adipose cells.

Wang and co-workers reported a imino-coumarin based probe **55** which showed strong blue emission in cells, indicating that probe has good cell membrane permeability and low cytotoxicity.¹³⁹ The colocalization coefficient and overlapping coefficient with MitoTracker Red CMXRos indicates that **55** localizes mainly within the mitochondria. Kawazoe *et al.* reported a probe **56** as mitochondrial surface specific indicator by carrying out double staining experiment on HeLa cells using MitoTracker Red.¹⁴⁰ Chemosensors **57a-c** containing dual mitochondrial targeting moieties have been developed by Cheng *et al.* as mitochondria targeting theranostic agents.¹⁴¹ Cellular images of **57a-c** and MitoTracker demonstrated the specific accumulation of these probes into the mitochondria of the tumor cells and can be used for the cancer cell fluorescence imaging. Parker *et al.* reported a europium complex **58** which selectively accumulated into the mitochondria of various cell lines, indicated by the colocalization experiments with Mitotracker Green.¹⁴² Similarly, Guo *et al.* developed copper-terpyridine complex **59** appended with mitochondrial targeting

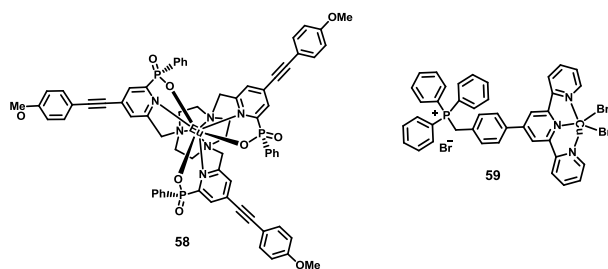


Fig. 24 Structures of compounds **58** and **59**.

unit as a potential anticancer agent.¹⁴³ Complex preferentially accumulated into the mitochondria of cell due the presence of triphenylphosphonium group and has more inhibition activity towards cancer cells. A variety of complexes and fluorescent probes have been reported recently by exploiting the phenomena of PET, AIE and two-photon fluorescence microscopy for mitochondrial imaging in living cells.¹⁴⁴ These probes possess specificity to the mitochondria, good photostability, cell permeability, lower cytotoxicity and also monitor mitochondrial dynamics.

Summary and future outlook

The present article discuss the recent developments in design and synthesis of mitochondrial targeting fluorescent probes and their particular applications to monitor the levels of ROS, metal ions, gasotransmitters, and thiols in biological systems as well as in solution. The synthetic strategy involves the utilization of mitochondrial specific functional units, namely TPP, pyridinium and imidazolium or delocalised positively charged fluorophores such as rhodamine, cyanines and metal complexes for efficient mitochondrial staining. From the overview discussed sections, we may conclude that the fluorescence imaging is simple and efficient method to visualize the changes occurs within the mitochondria of *cells in vivo* and *in vitro* due to the altered level of various species. Fluorophores like xanthene, BODIPY, cyanine, naphthalene, coumarin, and naphthalimide mounted with various reaction sites have been exploited for the mitochondrial detection process. But still there is a large space for the development of novel mitochondria targeted fluorescent probes for monitoring the pH, matrix viscosity, thiol, H₂S and other reactive oxygen and nitrogen species levels in cellular system.

Mitochondria are associated with cellular homeostasis by regulating metabolic activities, signal transduction and cell death. Likewise, the abnormalities in the mitochondrial functioning are responsible for different human disorders such as age-related diseases, cancer and cardiovascular disorders. The principal cause of mitochondrial defects is associated with the higher level of ROS generated during the oxidative phosphorylation and ATP production. For instance, oxidative stress state of the mitochondria due to the excess ROS has been related to the pathogenesis of Parkinson disease, hypertension, cancer and atherosclerosis. The information regarding the pathological state of the mitochondria will be significant to understand the mitochondrial abnormalities and to

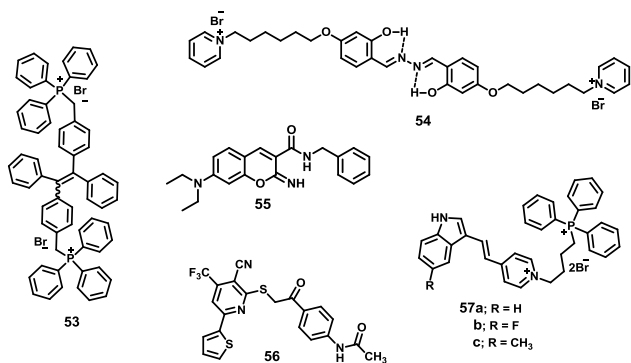


Fig. 23 Structures of compounds **53-57**.

implications of the succeeding therapeutic measures. Instead of extensive efforts in the area of mitochondrial related pathology, the present therapeutics is still less effective specifying the need of deep understanding in this area. In this context, fluorescent molecular probes, as discussed in this article, have potential to contribute to the understanding of mitochondrial related pathology and diseases. Thus, there is need to develop multi-functional fluorescent probes that are able to provide information about the different states of the mitochondria. For example, the information about the level of ROS and antioxidant enzyme systems are the important parameters related to the pathogenesis of mitochondria. Multi-functional fluorescent probes will be significant to achieve such challenging tasks. In addition, fluorescent probes can be advanced to monitor the selective targeting of drugs to the mitochondria as well as their action mechanisms, important for the effective therapeutic condition. Indeed, such advancements may be beneficial to control the mitochondrial impairment, to understand the pathology and to minimize the related disorders.

Acknowledgements

We are thankful to CSIR and DST for financial support. Guru Nanak Dev University for providing research facilities. We are also thankful to the researchers who contributed towards the development of mitochondrial targeting fluorogenic probes.

Notes and references

- K. Henze and W. Martin, *Nature*, 2003, **426**, 127.
- Y. L. P. Ow, D. R. Green, Z. Hao and T. W. Mak, *Nat. Rev. Mol. Cell Biol.*, 2008, **9**, 532.
- P. I. Moreira, X. Zhu, X. Wang, H.-g. Lee, A. Nunomura, R. B. Petersen, G. Perry and M. A. Smith, *Biochim. Biophys. Acta, Mol. Basis Dis.*, 2010, **1802**, 212.
- Y. Yamada and H. Harashima, *Adv. Drug Delivery Rev.*, 2008, **60**, 1439.
- D. C. Wallace, *Annu. Rev. Genet.*, 2005, **39**, 359.
- M. S. Remedi, C. G. Nichols and J. C. Koster, *Cell Metab.* 2006, **3**, 5.
- Y. I. Chen, A. M. Cypess, C. A. Sass, A. L. Brownell, K. T. Jokivarsi, C. R. Kahn and K. K. Kwong, *Obesity*, 2012, **20**, 1519.
- J. R. Lakowicz, *Principles of Fluorescence Spectroscopy*, 3rd ed., Springer, New York, 2006.
- H. N. Kim, W. X. Ren, J. S. Kim and J. Yoon, *Chem. Soc. Rev.*, 2012, **41**, 3210.
- S. A. Farber, M. Pack, S.-Y. Ho, I. D. Johnson, D. S. Wagner, R. Dosch, M. C. Mullins, H. S. Hendrickson, E. K. Hendrickson and M. K. Halpern, *Science*, 2001, **292**, 1385.
- L. D. Lavis and R. T. Raines, *ACS Chem. Biol.*, 2008, **3**, 142.
- H. M. Kim and B. R. Cho, *Acc. Chem. Res.*, 2009, **42**, 863.
- H. N. Kim, M. H. Lee, H. J. Kim, J. S. Kim and J. Yoon, *Chem. Soc. Rev.*, 2008, **37**, 1465.
- J. Wu, W. Liu, J. Ge, H. Zhang and P. Wang, *Chem. Soc. Rev.*, 2011, **40**, 3483.
- K. Kikuchi, *Chem. Soc. Rev.*, 2010, **39**, 2048.
- R. M. Duke, E. B. Veale, F. M. Pfeffer, P. E. Kruger and T. Gunnlaugsson, *Chem. Soc. Rev.*, 2010, **39**, 3936.
- R. Hu, N. L. C. Leung and B. Z. Tang, *Chem. Soc. Rev.*, 2014, **43**, 4494.
- X. Chen, T. Pradhan, F. Wang, J. S. Kim and J. Yoon, *Chem. Rev.*, 2012, **112**, 1910.
- Y. Yang, Q. Zhao, W. Feng and F. Li, *Chem. Rev.*, 2013, **13**, 192.
- J. S. M. Napolitano and J. R. Aprile, *Adv. Drug Deliv. Rev.* 2001, **49**, 63.
- M. P. Murphy, *Trends Biotechnol.*, 1997, **15**, 326.
- A. T. Hoye, J. E. Davoren, P. Wipf, M. P. Fink and V. E. Kagan, *Acc. Chem. Res.*, 2008, **41**, 87.
- J. Dessolin, M. Schuler, A. Quinart, F. De Giorgi, L. Ghose and F. Ichas, *Eur. J. Pharmacol.*, 2002, **447**, 155.
- A. Muratovska, R. N. Lightowlers, R. W. Taylor, J. A. Wilcox and M. P. Murphy, *Adv. Drug Deliv. Rev.*, 2001, **49**, 189.
- L. B. Chen, *Annu. Rev. Cell Biol.*, 1988, **4**, 155.
- E. Bussalleu, E. Pinart, M. Yeste, M. Briz, S. Sancho, N. Garcia-Gil, E. Badia, J. Bassols, A. Pruneda, I. Casas and S. Bone, *Microsc. Res. Tech.*, 2005, **68**, 277.
- A. V. Kuznetsov, M. Hermann, J. Troppmair, R. Margreiter, I. Hengster, *J. Cell. Mol. Med.*, 2010, **14**, 417.
- K. Dobashi, B. Ghosh, J. K. Orak, I. Singh and A. K. Singh, *Mol. Cell. Biol.*, 2000, **20**, 1.
- K. N. Schmidt, P. Amstad, P. Cerutti and P. A. Baeuerle, *Chem. Biol.*, 1995, **2**, 13.
- F. J. Turrens, *J. Physiol.*, 2003, **552**, 335.
- B. C. Dickinson and C. J. Chang, *Nat. Chem. Biol.*, 2011, **7**, 504.
- M. P. Murphy, *Biochem. J.*, 2009, **417**, 1.
- E. A. Veal, A. M. Day and B. A. Morgan, *Mol. Cell*, 2007, **26**, 1.
- Z. M. Prokopowicz, F. Arce, R. Biedron, C. L.-L. Chiang, M. Cizek, D. R. Katz, M. Nowakowska, S. Zapotoczny, J. Marcinkiewicz and B. M. Chain, *J. Immunol.*, 2010, **184**, 824.
- A. Daugherty, J. L. Dunn, D. L. Rateri and J. W. Heinecke, *J. Clin. Invest.*, 1994, **94**, 437.
- S. M. Wu and S. V. Pizzo, *Arch Biochem. Biophys.*, 2001, **397**, 119.
- Y. Koide, Y. Urano, S. Kenmoku, H. Kojima and T. Nagano, *J. Am. Chem. Soc.*, 2007, **129**, 10324.
- B. C. Dickinson and C. J. Chang, *J. Am. Chem. Soc.*, 2008, **130**, 9638.
- W. Denk, J. H. Strickler and W. W. Webb, *Science*, 1990, **248**, 73.
- G. Masanta, C. H. Heo, C. S. Lim, S. K. Bae, B. R. Cho and I. M. Kim, *Chem. Commun.*, 2012, **48**, 3518.
- P. Li, W. Zhang, K. Li, X. Liu, H. Xiao, W. Zhang and B. Tang, *Anal. Chem.*, 2013, **85**, 9877.
- J.-T. Hou, M.-Y. Wu, K. Li, J. Yang, K.-K. Yu, Y.-M. Xie and X.-Q. Yu, *Chem. Commun.*, 2014, **50**, 8640.
- J.-T. Hou, K. Li, J. Yang, K.-K. Yu, Y.-X. Liao, Y.-Z. Ran, Y.-H. Liu, X.-D. Zhou and X.-Q. Yu, *Chem. Commun.*, 2015, **51**, 6781.
- G. Cheng, J. Fan, W. Sun, K. Sui, X. Jin, J. Wang and X. Peng, *Analyst*, 2013, **138**, 6091.
- G. Li, Q. Lin, L. Ji and H. Chao, *J. Mater. Chem. B*, 2014, **2**, 7918.
- H. Xiao, K. Xin, H. Dou, G. Yin, Y. Quan and R. Wang, *Chem. Commun.*, 2015, **51**, 1442.
- H. Xiao, J. Li, J. Zhao, G. Yin, Y. Quan, J. Wang and R. Wang, *J. Mater. Chem. B*, 2015, **3**, 1633.
- L. Yuan, L. Wang, B. K. Agrawalla, S.-J. Park, H. Zhu, B. Sivaraman, J. Peng, Q.-H. Xu and Y.-T. Chang, *J. Am. Chem. Soc.*, 2015, **137**, 5930.
- H. Zhang, J. Liu, Y.-Q. Sun, Y. Huo, Y. Li, W. Liu, X. Wu, N. Zhang, Y. Shi and W. Guo, *Chem. Commun.*, 2015, **51**, 2721.
- F. Yu, P. Li, B. Wang and K. Han, *J. Am. Chem. Soc.*, 2013, **135**, 7674.
- J. Qiao, Z. Liu, Y. Tian, M. Wu and Z. Niu, *Chem. Commun.*, 2015, **51**, 3641.
- R. Lill, *Nature*, 2009, **460**, 831.
- R. S. Ajioka, J. D. Phillips, J. P. Kushner, *Biochim. Biophys. Acta*, 2006, **1763**, 723.

- 54 J. Silvia, R. Williams, *The Biological Chemistry of the Elements: The Inorganic Chemistry of Life*, Clarendon Press, Oxford, 1991.
- 55 M. L.-H. Huang, E. M. Becker, M. Whitnall, Y. S. Rahmanto, P. Ponka, and D. R. Richardson, *Proc. Natl. Acad. Sci. U. S. A.*, 2009, **106**, 16381.
- 56 M. L.-H. Huang, D. J. R. Lane and D. R. Richardson, *Antioxid. Redox Signaling*, 2011, **15**, 3003.
- 57 W.-d. Chen, W.-t. Gong, Z.-q. Ye, Y. Lin and G.-l. Ning, *Dalton Trans.*, 2013, **42**, 10093.
- 58 J. M. Berg and Y. Shi, *Science*, 1996, **271**, 1081.
- 59 R. Colvin, W. Holmes, C. Fontaine and W. Maret, *Metallomics*, 2010, **2**, 306.
- 60 A. Krezel and W. Maret, *J. Biol. Inorg. Chem.*, 2006, **11**, 1049.
- 61 S. L. Kelleher, N. H. McCormick, V. Velasquez and V. Lopez, *Adv. Nutr.*, 2011, **2**, 101.
- 62 S. L. Sensi, H. Z. Yin and J. H. Weiss, *Eur. J. Neurosci.* 2000, **12**, 3813.
- 63 S. L. Sensi, P. Paoletti, A. I. Bush, I. Sekler, *Nat. Rev. Neurosci.*, 2009, **10**, 780.
- 64 K. Sreenath, J. R. Allen, M. W. Davidson and L. Zhu, *Chem. Commun.*, 2011, **47**, 11730.
- 65 L. Xue, G. Li, C. Yu and H. Jiang, *Chem. Eur. J.*, 2012, **18**, 1050.
- 66 G. Masanta, C. S. Lim, H. J. Kim, J. H. Han, H. M. Kim and B. R. Cho, *J. Am. Chem. Soc.*, 2011, **133**, 5698.
- 67 N. Y. Baek, C. H. Heo, C. S. Lim, G. Masanta, B. R. Cho and H. M. Kim, *Chem. Commun.*, 2012, **48**, 4546.
- 68 K. Rathore, C. S. Lim, Y. Lee and B. R. Cho, *Org. Biomol. Chem.*, 2014, **12**, 3406.
- 69 W. Chyan, D. Y. Zhang, S. J. Lippard and R. J. Radford, *Proc. Natl. Acad. Sci. U. S. A.*, 2014, **111**, 143.
- 70 A. Loas, R. J. Radford and S. J. Lippard, *Inorg. Chem.*, 2014, **53**, 6491.
- 71 C. M. Troy, L. Stefanis, A. Prochiantz, L. A. Greene and M. L. Shelanski, *Proc. Natl. Acad. Sci. U. S. A.*, 1996, **93**, 5635.
- 72 M. Taki, K. Akaoka, K. Mitsui and Y. Yamamoto, *Org. Biomol. Chem.*, 2014, **12**, 4999.
- 73 S. C. Dodani, S. C. Leary, P. A. Cobine, D. R. Winge and C. J. Chang, *J. Am. Chem. Soc.*, 2011, **133**, 8606.
- 74 W. K. Alderton, C. E. Cooper and R. G. Knowles, *Biochem. J.*, 2001, **357**, 593.
- 75 A. Soneja, M. Drews and T. Malinski, *Pharmacol. Rep.*, 2005, **57(suppl)**, 108.
- 76 S. H. Snyder, *Science*, 1992, **257**, 494.
- 77 D. Fukumura, S. Kashiwagi and R. K. Jain, *Nat. Rev. Cancer*, 2006, **6**, 521.
- 78 F. Pricci, G. Leto, L. Amadio, C. Iacobini, S. Cordone, S. Catalano, A. Zicari, M. Sorcini, U. R. Di Mario and G. Pugliese, *Free Radical Biol. Med.*, 2003, **35**, 683.
- 79 N. Kumar, V. Bhalla and M. Kumar, *Coord. Chem. Rev.*, 2013, **257**, 2335.
- 80 E. Nisoli and M. O. Carruba, *J. Cell Sci.*, 2006, **119**, 2855.
- 81 H. Yu, X. Zhang, Y. Xiao, W. Zou, L. Wang and L. Jin, *Anal. Chem.*, 2013, **85**, 7076.
- 82 E. Sasaki, H. Kijima, H. Nishimatsu, Y. Urano, K. Kikuchi, Y. Hirata and T. Nagano, *J. Am. Chem. Soc.*, 2005, **127**, 3684.
- 83 T. Terai, Y. Urano, S. Izumi, H. Hojima and T. Nagano, *Chem. Commun.*, 2012, **48**, 2840.
- 84 C. Yu, Y. Wu, F. Zeng, S. Wu, *J. Mater. Chem. B*, 2013, **1**, 4152.
- 85 Y.-Q. Sun, J. Liu, H. Zhang, Y. Huo, X. Lv, Y. Shi and W. Guo, *J. Am. Chem. Soc.*, 2014, **136**, 12520.
- 86 X. Chen, L. Sun, Y. Chen, X. Cheng, W. Wu, L. Ji and H. Chao, *Biomaterials*, 2015, **58**, 72.
- 87 J. E. Dominy and M. H. Stipanuk, *Nutr. Rev.*, 2004, **62**, 348.
- 88 M. M. Gadalla and S. H. Snyder, *J. Neurochem.*, 2010, **113**, 14.
- 89 P. Kamoun, *Med. Hypotheses*, 2001, **57**, 389.
- 90 J. L. Wallace and R. Wang, *Nat. Rev. Drug. Discov.*, 2015, **14**, 329.
- 91 Y. Chen, C. Zhu, Z. Yang, J. Chen, Y. He, Y. Jiao, W. He, L. Qiu, J. Cen and Z. Guo, *Angew. Chem. Int. Ed.*, 2013, **52**, 1688.
- 92 X. Wang, J. Sun, W. Zhang, X. Ma, J. Lv and B. Tang, *Chem. Sci.*, 2013, **4**, 2551.
- 93 M. Gao, F. Yu, H. Chen and L. Chen, *Anal. Chem.*, 2015, **87**, 3631.
- 94 X.-L. Liu, X.-J. Du, C.-G. Dai and Q.-H. Song, *J. Org. Chem.*, 2014, **79**, 9481.
- 95 J. Bouffard, Y. Kim, T. M. Swager, R. Weissleder and S. J. Hilderbrand, *Org. Lett.*, 2008, **10**, 37.
- 96 M. Marí, A. Morales, A. Colell, C. García-Ruiz, J. C. Fernández-Checa, *Antioxid. Redox Signaling*, 2009, **11**, 2685.
- 97 K. Shioji, H. Nakamura, H. Masutani and J. Yodoi, *Antioxid. Redox Signal.*, 2003, **5**, 795.
- 98 I. Csiki, K. Yanagisawa, N. Haruki, S. Nadaf, J. D. Morrow, L. H. Johnson and D. P. Carbone, *Cancer Res.*, 2006, **66**, 143.
- 99 Y. Matsuo and J. Yodoi, *Cytokine Growth Factor Rev.*, 2011, **24**, 345.
- 100 C. S. Lim, G. Masanta, H. J. Kim, J. H. Han, H. M. Kim and B. R. Cho, *J. Am. Chem. Soc.*, 2011, **133**, 11132.
- 101 S.-Y. Lim, K.-H. Hong, D. I. Kim, H. Kwon and H.-J. Kim, *J. Am. Chem. Soc.*, 2014, **136**, 7018.
- 102 M. H. Lee, J. H. Han, J.-H. Lee, H. G. Choi, C. Kang and J. S. Kim, *J. Am. Chem. Soc.*, 2012, **134**, 17314.
- 103 A. Ishaque and M. J. Al-Rubeai, *Immunol. Methods*, 1998, **221**, 43.
- 104 A. Varadi and G. A. Rutter, *Endocrinology*, 2004, **144**, 4540.
- 105 E. Liang, P. Liu and S. Dinh, *Int. J. Pharm.*, 2007, **338**, 104.
- 106 K. R. Hoyt and I. J. Reynolds, *J. Neurochem.*, 1998, **71**, 1051.
- 107 L. F. Yousif, K. M. Stewart and S. O. Kelley, *Chem Biochem*, 2009, **10**, 1939.
- 108 H. I. Gursahani and S. Schaefer, *Am. J. Physiol.: Heart Circ. Physiol.*, 2004, **287**, H2659.
- 109 C. Balut, M. vande Ven, S. Despa, I. Lambrichts, M. Ameloot, P. Steels and I. Smets, *Kidney Int.*, 2008, **73**, 226.
- 110 E. Chacon, J. M. Reece, A.-L. Nieminen, G. Zahrebelski, J. Herman and J. J. Lemasters, *Biophys. J.*, 1994, **66**, 942.
- 111 M. F. C. Abad, G. Di Benedetto, P. J. Magalhaes, L. Filippini and T. Pozzan, *J. Biol. Chem.*, 2004, **279**, 11521.
- 112 A. M. Porcelli, A. Ghelli, C. Zanna, P. Pinton, R. Rizzuto and M. Rugolo, *Biochem. Biophys. Res. Commun.*, 2005, **326**, 799.
- 113 M. Tantama, Y. P. Hung and G. Yellen, *J. Am. Chem. Soc.*, 2011, **133**, 10034.
- 114 M. H. Lee, N. Park, C. Yi, J. H. Han, J. H. Hong, K. P. Kim, F. H. Kang, J. L. Sessler, C. Kang and J. S. Kim, *J. Am. Chem. Soc.*, 2014, **136**, 14136.
- 115 P. Li, H. Xiao, Y. Cheng, W. Zhang, F. Huang, W. Zhang, L. Wang and B. Tang, *Chem. Commun.*, 2014, **50**, 7184.
- 116 M. J. Stutts, C. M. Canessa, J. C. Olsen, M. Hamrick, J. A. Cohn, B. C. Rossier and R. C. Boucher, *Science*, 1995, **268**, 847.
- 117 O. G. Luneva, N. A. Brazhe, N. V. Maksimova, O. V. Rodnenkov, E. Y. Parsina, N. Y. Bryzgalova, G. V. Maksimov, A. B. Rubin, S. N. Orlov and E. I. Chazov, *Pathophysiology*, 2007, **14**, 41.
- 118 J. S. Goodwin, K. R. Drake, C. L. Remment and A. K. Kenworthy, *Biophys. J.*, 2005, **89**, 1398.
- 119 A. Kearney-Schwartz, J. M. Virion, J.-F. Stoltz, P. Drouot and F. Zannad, *Fund. Clin. Pharmacol.* 2007, **21**, 387.
- 120 S. J. Singer and G. L. Nicolson, *Science*, 1972, **175**, 720.
- 121 Z. Yang, Y. He, J.-H. Lee, N. Park, M. Suh, W.-S. Chae, J. Cao, X. Peng, H. Jung, C. Kang and J. S. Kim, *J. Am. Chem. Soc.*, 2013, **135**, 9181.

- 122 F. Liu, T. Wu, J. Cao, S. Cui, Z. Yang, X. Qiang, S. Sun, F. Song, J. Fan, J. Wang and X. Peng, *Chem. Eur. J.*, 2013, **19**, 1548.
- 123 N. Jiang, J. Fan, S. Zhang, T. Wua, J. Wang, P. Gaob, J. Qu, F. Zhou and X. Peng, *Sens. Actuators, B*, 2014, **190**, 685.
- 124 H. Bayir, V. A. Tyurin, Y. Y. Tyurina, R. Viner, V. Ritov, A. A. Amoscato, Q. Zhao, X. J. Zhang, K. L. Janesko-Feldman, H. Alexander, L. V. Basova, R. S. Clark, P. M. Kochanek and V. E. Kagan, *Ann. Neurol.*, 2007, **62**, 154.
- 125 T. A. Prime, M. Forkink, A. Logan, P. G. Finichiu, J. McLachlan, P. B. L. Pun, W. J. H. Koopman, L. Larsen, M. J. Latter, R. A. J. Smith and M. P. Murphy, *Free Radical Biol. Med.*, 2012, **53**, 544.
- 126 R. Blaylock, *Fluoride*, 2004, **37**, 301.
- 127 S. Zhang, J. Fan, S. Zhang, J. Wang, X. Wang, J. Du and X. Peng, *Chem. Commun.*, 2014, **50**, 14021.
- 128 Y. Liu, K. Li, M.-Y. Wu, Y.-H. Liu, Y.-M. Xie and X.-Q. Yu, *Chem. Commun.*, 2015, **51**, 10236.
- 129 N. Denora, V. Laquintana, A. Trapani, H. Suzuki, M. Sawada and G. Trapani, *Pharm. Res.*, 2011, **28**, 2820.
- 130 M. Homma, Y. Takei, A. Murata, T. Inoue and S. Takeoka, *Chem. Commun.*, 2015, **51**, 6194.
- 131 N. Jiang, J. Fan, F. Xu, X. Peng, H. Mu, J. Wang and X. Xiong, *Angew. Chem. Int. Ed.*, 2015, **54**, 2510.
- 132 W. Yang, P. S. Chan, M. S. Chan, K. F. Li, P. K. Lo, N. K. Mak, K. W. Cheah and M. S. Wong, *Chem. Commun.*, 2013, **49**, 3428.
- 133 A. R. Sarkar, C. H. Heo, H. W. Lee, K. H. Park, Y. H. Suh and H. M. Kim, *Anal. Chem.*, 2014, **86**, 5638.
- 134 F. Miao, W. Zhang, Y. Sun, R. Zhang, Y. Liu, F. Guo, G. Song, M. Tian and X. Yu, *Biosens. Bioelectron.*, 2014, **55**, 423.
- 135 X. Zhang, Y. Xiao, J. Qi, J. Qu, B. Kim, X. Yue and K. D. Belfield, *J. Org. Chem.*, 2013, **78**, 9153.
- 136 B. Wang, Y. Wang, H. Wu, X. Song, X. Guo, D. Zhang, X. Ma and M. Tan, *RSC Adv.*, 2014, **4**, 49960.
- 137 C. W. T. Leung, Y. Hong, S. Chen, E. Zhao, J. W. Y. Lam and B. Z. Tang, *J. Am. Chem. Soc.*, 2013, **135**, 62.
- 138 M. Gao, C. K. Sim, C. W. T. Leung, Q. Hu, G. Feng, F. Xu, B. Z. Tang and B. Liu, *Chem. Commun.*, 2014, **50**, 8312.
- 139 D. Guo, T. Chen, D. Ye, J. Xu, H. Jiang, K. Chen, H. Wang and H. Liu, *Org. Lett.*, 2011, **13**, 2884.
- 140 Y. Kawazoe, H. Shimogawa, A. Sato and M. Uesugi, *Angew. Chem. Int. Ed.*, 2011, **50**, 5478.
- 141 S. Wu, Q. Cao, X. Wang, K. Cheng and Z. Cheng, *Chem. Commun.*, 2014, **50**, 8919.
- 142 J. W. Walton, A. Bourdolle, S. J. Butler, M. Soulie, M. Delbianco, B. K. McMahon, R. Pal, H. Puschmann, J. M. Zwier, L. Lamarque, O. Maury, C. Andraud and D. Parker, *Chem. Commun.*, 2013, **49**, 1600.
- 143 W. Zhou, X. Wang, M. Hu, C. Zhu and Z. Guo, *Chem. Sci.*, 2014, **5**, 2761.
- 144 S. Huang, R. Han, Q. Zhuang, L. Du, H. Jia, Y. Liu and Y. Liu, *Biosensors and Bioelectronics*, 2015, **71**, 313.
- 145 C.-J. Zhang, Q. Hu, G. Feng, R. Zhang, Y. Yuan, X. Lu and B. Liu, *Chem. Sci.*, 2015, **6**, 4580.
- 146 B. Liu, M. Shah, G. Zhang, Q. Liu and Y. Pang, *ACS Appl. Mater. Interfaces*, 2014, **6**, 21638.
- 147 P. H. P. R. Carvalho, J. R. Correa, B. C. Guido, C. C. Gatto, H. C. B. De Oliveira, T. A. Soares and B. A. D. Neto, *Chem. Eur. J.*, 2014, **20**, 15360.
- 148 A. L. Capodilupo, V. Vergaro, E. Fabiano, M. De Giorgi, F. Baldassarre, A. Cardone, A. Maggiore, V. Maiorano, D. Sanvitto, G. Gigli and G. Ciccarella, *J. Mater. Chem. B.*, 2015, **3**, 3315.
- 149 M. Grzybowski, E. G.-Mrowka, V. Hugues, W. Brutkowski, M. B.-Desce and D. T. Gryko, *Chem. Eur. J.*, 2015, **21**, 9101.
- 150 W. Zhang, R. T. K. Kwok, Y. Chen, S. Chen, E. Zhao, C. Yu, J. W. Y. Lam, Q. Zheng and B. Z. Tang, *Chem. Commun.*, 2015, **51**, 9022.
- 151 Q. Hu, M. Gao, G. Feng and B. Liu, *Angew. Chem. Int. Ed.*, 2014, **53**, 14225.
- 152 Y. Chen, W. Xu, J. Zuo, L. Ji and H. Chao, *J. Mater. Chem. B*, 2015, **3**, 3306.